Inorganic Chemistry

Article

pubs.acs.org/IC

Does the Oxidation of Nitric Oxide by oxyMyoglobin Share an Intermediate with the metMyoglobin-Catalyzed Isomerization of Peroxynitrite?

Karl J. Koebke, Daniel J. Pauly, Leonid Lerner, Xien Liu,[†] and A. Andrew Pacheco*

Department of Chemistry and Biochemistry, University of Wisconsin−Milwaukee, Milwaukee, Wisconsin 53211, United States

Supporting Information

ABSTRACT: The reaction of nitric oxide with oxy-myoglobin (oxyMb) to form ferric myoglobin (metMb) and nitrate, and the metMb-catalyzed isomerization of peroxynitrite to nitrate, have long been assumed to proceed via the same iron-bound peroxynitrite intermediate (metMb(OONO)). More recent research showed that the metMb-catalyzed isomerization of peroxynitrite to nitrate produces detectable amounts of nitrogen dioxide and ferryl myoglobin (ferrylMb). This suggests a mechanism in which the peroxynitrite binds to the metMb, ferrylMb is transiently generated by dissociation of NO_2, and nitrate is formed when the NO_2 nitrogen attacks the ferrylMb oxo ligand. The presence of free NO_2 and ferrylMb products reveals that small amounts of NO_2 escape from myoglobin's interior before recombination can occur. Free NO_2 and ferrylMb should also be generated in the reaction of oxyMb with NO, if the common intermediate metMb(OONO) is formed. However, this report presents a series of time-resolved UV/vis spectroscopy experiments in which no ferrylMb was detected when oxyMb and NO reacted. The sensitivity of the methodology is such that as little as 10% of the ferrylMb predicted from the experiments with metMb and peroxynitrite should have been detectable. These results lead to the conclusion that the oxyMb + NO and metMb + $ONOO^-$ reactions do *not* proceed via a common intermediate as previously thought. The conclusion has significant implications for researchers that propose a possible role of oxyMb in intracellular NO regulation, because it means that toxic NO_2 and ferrylMb are not generated during NO oxidation by this species.

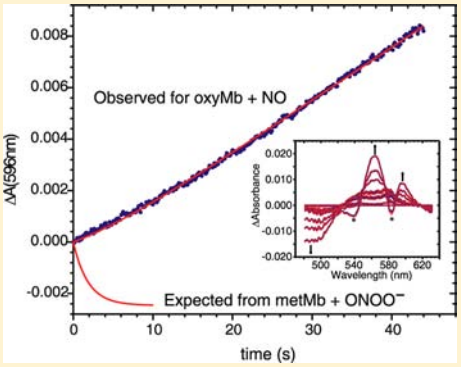

INTRODUCTION

Myoglobin's role as an oxygen storage protein in tissues is widely accepted,[1,2] despite some studies demonstrating that myoglobin-deficient mice have apparently normal muscle function.[3] Nevertheless, in recent years many researchers have suggested that the protein may also serve a variety of other physiological functions.[4−7] One such function is as a NO sink. In this case, oxy-myoglobin (oxyMb) reacts with NO to release nitrate, leaving the myoglobin in an aquated ferric state known as aquomet-myoglobin (metMb) (Scheme 1).[4,5,8] Nitric oxide plays many important physiological roles as a signaling molecule,[9,10] all of which take advantage of its transient nature. Thus, the reaction of Scheme 1 could serve to spatially limit the range of a NO signal within tissues that contain high concentrations of myglobin, such as cardiac and skeletal muscles, and to keep the concentration of NO within the cell below toxic levels.[4]

The first step in the reaction of oxyMb with NO is commonly accepted to be the formation of a peroxynitrite-bound intermediate (metMb(OONO)), as shown in Scheme 1,[11,12] though it should be noted that such an intermediate has never been directly detected. At alkaline pH an intermediate was detected in UV/vis stopped-flow[8] and rapid freeze-quench EPR[13] studies, that at first was believed to be the peroxynitrite species. However, an intermediate species with identical kinetic behavior was later detected in the reaction of ferrylMb with NO_2, and identified as the metMb(ONO_2) adduct (Scheme 1).[14] Very recently this assignment was confirmed using rapid freeze-quench resonance Raman spectroscopic analysis.[15] One indirect piece of evidence for the intermediacy of metMb-(OONO) is that metMb and related proteins can catalyze the isomerization of peroxynitrite to nitrate, presumably through the same intermediate, as shown in refs 16−19. Model studies with synthetic porphyrins by Schopfer et al. provide additional indirect evidence.[20]

Though a peroxynitrite intermediate is generally assumed in the reaction of oxyMb with NO, there has been less agreement on the mechanism by which this intermediate rearranges to the nitrate adduct (metMb(ONO_2)), with some researchers favoring a concerted rearrangement (Scheme 1, path 1),[18,21] and others an O−O bond homolysis to generate a ferryl myoglobin (ferrylMb) intermediate and NO_2, followed by a recombination in which the N of NO_2 binds to the ferryl oxo group (Scheme 1, path 2).[15,17,19,20] Over the past decade though, a series of experiments that followed the reaction of peroxynitrite with metMb has provided persuasive evidence that the metMb(OONO) adduct rearranges according to the

Received: March 20, 2013
Published: June 14, 2013

   dx.doi.org/10.1021/ic400697a | *Inorg. Chem.* 2013, 52, 7623−7632

Scheme 1

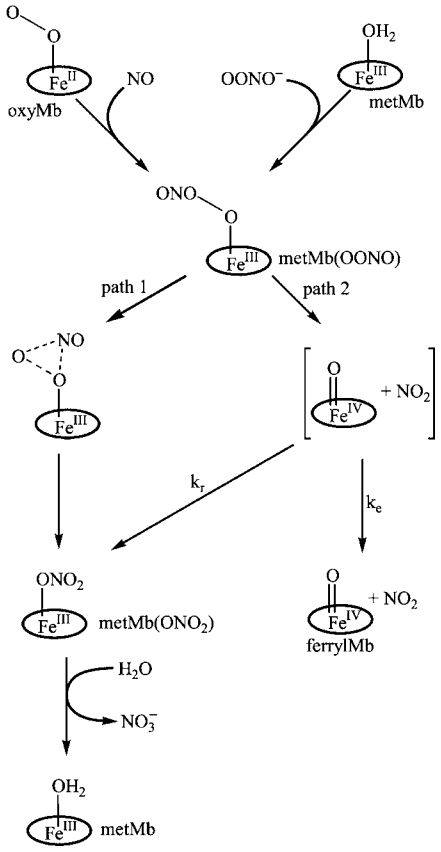

path 2 homolysis model. The culmination came in a recent paper where Su and Groves were able to directly detect the putative ferrylMb intermediate.[19] This and earlier papers also reported the nitration of a specific tyrosine within Mb (Tyr103), presumably by NO_2 generated from the peroxynitrite fragmentation and lost through the cage escape pathway (Scheme 1, lower-right).[17,19] With the chemistry of the metMb(OONO) species now fairly well established, this paper revisits the question of whether this species in fact represents a common intermediate when oxyMb reacts with NO, and when metMb reacts with peroxynitrite.

MATERIALS AND METHODS

All reagents were purchased from Sigma-Aldrich or Fisher Scientific unless otherwise specified. The light-activated NO precursor [Mn(PaPy$_2$Q)NO]ClO$_4$ (Scheme 2, species **1**, where PaPy$_2$Q is the pentadentate ligand *N*,*N*-bis(2-pyridylmethyl)-amine-*N*-ethyl-2-quinoline-2-carboxamide) and the pH-jump activated NO precursor 1-(*N*,*N*-diethylamino)diazene-1-ium-1,2-diolate (DEANO)[22] were prepared by the methods of Eroy-Reveles et al.[23] and Drago and Paulik,[24,25] respectively. Horse-heart myoglobin as obtained from Sigma was in the metMb form. This was reduced in a glovebox using an excess of electrolytically generated methyl viologen monocation radical[26] to generate ferromyoglobin (Mb), which could in turn be converted to oxyMb by exposure to ambient air. FerrylMb was generated by exposing metMb to excess hydrogen peroxide, which was then removed by adding ~10^{-8} M catalase, as previously described.[19] Nitrosylated metMb (metMbNO) and Mb (MbNO) were prepared by exposing metMb and Mb, respectively, to NO gas generated in situ from DEANO.[24,25] Extinction coefficient spectra were obtained for all the above-mentioned forms of myoglobin.

All experiments described herein were carried out in solutions buffered at pH 7.4 using HEPES and made using 18 MΩ purified water. Stock solutions of most reagents were made up in 50 mM HEPES. In the case of ascorbate, a 1.25 M stock solution was made by dissolving 5.5 g of ascorbic acid and 7.45 g of HEPES sodium salt in 50 mL of water and then adjusting the pH to 7.4 with NaOH or HCl, as appropriate. Reaction mixtures were made by combining appropriate volumes of the stock solutions. Routine UV/vis spectra were obtained using CARY 50 spectrophotometers (Varian); an instrument installed in the glovebox was available for air-sensitive measurements. Photochemical fragmentation of species **1** was initiated with 10 ns, 500 nm laser pulses generated using an OPO tunable laser (Opotec Rainbow Vis). An OLIS RSM-1000 spectrophotometer was used to monitor the absorbance changes induced in the reaction mixture by the laser pulse. The configuration of the laser and spectrophotometric equipment was as described in general terms elsewhere,[27,28] except that the laser pulse was transmitted via an optical fiber instead of by using mirrors. Reactions with lifetimes of less than 2 ms were monitored with the OLIS RSM-1000 in fixed wavelength mode. Data arrays that tracked the changes in the complete spectra as a function of time were then constructed from multiple absorbance vs time traces collected for the same reaction at varying wavelengths. For reactions with lifetimes higher than 2 ms, data were collected with the OLIS RSM-1000 in rapid-scanning average 1 mode, which provides 62 scans/s (1 scan every 16 ms). After verifying that no significant changes were occurring on the millisecond time scale, the raw spectra were further averaged to obtain spectra spaced 160 ms apart. For all experiments, the solutions were held in 1.5 mm × 1.5 mm fluorometer submicro cuvettes (Starna). The laser pulse was focused as a spot of ~5 mm diameter which irradiated the entire cuvette window. The laser pulse energies were measured before and after each day's experiments using a Scientech AC2501 bolometer; typical pulse energy intensities at the cuvette were ~15−18 mJ/cm^2.

All data were analyzed using programs written within the commercially available software packages Origin version 6.0 (Microcal Software) or Mathcad 13 (PTC Software). The analysis strategies used in our laboratories have been previously described;[22,28−31] details specific to this work are provided as Supporting Information.

Scheme 2

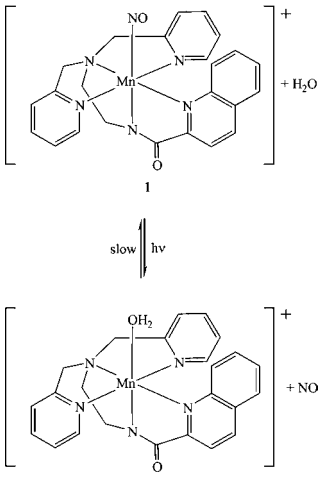

RESULTS

In this study, NO was generated photochemically by irradiating the photoactive manganese nitrosyl complex **1** (Scheme 2).[23] When species **1** is irradiated with a 500 nm, 10 ns laser pulse, it fragments in less than 1 μs to release free NO and an aqua-substituted product of **1**, as shown in Scheme 2. This is a very convenient way of generating NO in an aerobic solution of oxyMb, because under the reaction conditions free NO is in contact with free oxygen for less than 0.5 ms before it is all consumed in the reaction with oxyMb.[8] Thus, unwanted side-reactions, particularly the formation of NO_2 from direct

dx.doi.org/10.1021/ic400697a | Inorg. Chem. 2013, 52, 7623−7632

interaction between NO and O_2, are easily avoided. For the purposes of the present study, species **1** is superior to other known NO photoprecursors for two reasons. First, the NO can be generated in large quantities (as high as 150 μM in the present study) using long-wavelength light (500 nm or longer); other high-yield NO photoprecursors that were used in the past by this research group require UV laser pulses.[28] Second, the aquated photoproduct of **1** is not very reactive on the time scales being investigated, as is verified in experiments described below. Many other NO photoprecursors fragment to yield products that are either strong oxidants[28] or strong reductants,[32,33] which can take part in side-reactions on the time scales of interest, thus complicating their use in experiments.

Experiments with No Ascorbate Added. Figure 1 shows the difference spectrum obtained immediately after irradiating a solution of 316 μM oxyMb and 1.66 mM **1** with a 500 nm laser pulse. The Figure 1 difference spectrum can be fitted reasonably well using the independently known extinction coefficients of metMb, oxyMb, **1**, and ferrylMb (Figure 1, red dashed trace). On the basis of this fit, the changes in concentrations of the various species are calculated to be ΔC_{metMb} = 81 μM, ΔC_{oxyMb} = ΔC_1 = −86 μM, and $\Delta C_{ferrylMb}$ = 5 μM. Note however that this method is quite insensitive, and a similar fit can be obtained using the extinction coefficients of metMb, oxyMb, **1**, and Mb (Figure 1, green dashed trace). In this case, the calculated concentrations of the species are ΔC_{metMb} = $-\Delta C_1$ = 82 μM, ΔC_{oxyMb}= −86 μM, and ΔC_{Mb} = 4 μM. Neither fit is improved by adding in contributions from the extinction coefficient spectrum of MbNO. The presence of either ferrylMb or Mb is mechanistically plausible: if a peroxynitrite intermediate is formed from the reaction of oxyMb with NO, then ferrylMb is an expected product.[19] On the other hand, the rapid reaction of oxyMb with NO also consumes O_2, thus perturbing the equilibrium between oxyMb, free Mb, and dissolved O_2.

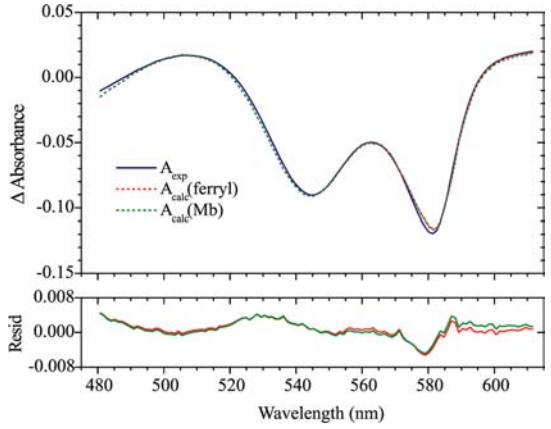

Figure 1. Difference spectrum obtained immediately after irradiating a solution of 316 μM oxyMb and 1.66 mM **1** with a 500 nm laser pulse. Solid blue trace: experimentally obtained data. Dashed red trace: calculated by least-squares fit using the extinction coefficient spectra of oxyMb, metMb, ferrylMb, and **1**. Dashed green trace: same as red trace but using the Mb extinction coefficient spectrum instead of the ferrylMb one. The fitted experimental spectrum was the average of the first 20 raw spectra collected every 16 ms using the Olis spectrophotometer (absorbance remained essentially constant throughout this time period, which allowed for signal averaging).

If one accepts the hypothesis that the same metMb(OONO) intermediate is generated in the reaction of oxyMb with NO and in the metMb-catalyzed isomerization of peroxynitrite (Scheme 1), then it is possible to estimate the expected final product distribution using only kinetic parameters available in the literature.[8,14,19,34−36] The relevant reactions, together with the associated kinetic parameters and the source references, are shown in Scheme 3. Su and Groves estimated that the rate for

Scheme 3[a]

oxyMb + NO → metMb + NO_3^-	k_{11} =(3.87±0.05)x10^7 $M^{-1}s^{-1}$ (a)
oxyMb + NO → ferrylMb + NO_2	k_{12} =(4.30±0.05)x10^6 $M^{-1}s^{-1}$ (a)
ferrylMb + NO → metMb + NO_2^-	k_2 =(1.80±0.05)x10^7 $M^{-1}s^{-1}$ (b)
metMb + NO → metMbNO	k_3 =(4.8±0.3)x10^4 $M^{-1}s^{-1}$ (c)
oxyMb + NO_2 → $ferrylMb^{+\bullet}$ + NO_3^-	k_4 =(4.5±0.3)x10^7 $M^{-1}s^{-1}$ (d)
ferrylMb + NO_2 → metMb + NO_3^-	k_5 = (1.2±0.3)x10^7 $M^{-1}s^{-1}$ (d)
$ferrylMb^{+\bullet}$ + oxyMb → ferrylMb + metMb	k_6=10^4-10^7 $M^{-1}s^{-1}$ (d)
ferrylMb + oxyMb → 2metMb	k_7 = 21±5 $M^{-1}s^{-1}$ (d)
NO + NO_2 ⇌ N_2O_3	k_8 = 1.1x10^9 $M^{-1}s^{-1}$ (d,e) k_{-8} = 8.1x10^4 s^{-1} (d,e)
N_2O_3 + H_2O → $2NO_2^-$ + $2H^+$	k_9 = 2000 s^{-1} (pH 7)(e)

[a]References for the rate constants are as follows: (a) refs 8 and 19; (b) ref 35; (c) ref 36.; (d) ref 14; (e) ref 34.

in-cage recombination of NO_2 and ferrylMb to form metMb-(ONO_2) is ∼10× that of cage escape by NO_2 (k_r/k_e ∼ 10 in Scheme 1).[19] For the reaction that gave rise to the Figure 1 results, in which ∼86 μM of oxyMb reacted with an equivalent amount of photogenerated NO, this would mean that initially about 8 μM ferrylMb, 8 μM free NO_2, and 78 μM metMb should have been generated. This estimate of ferrylMb generated is about twice that calculated in the red trace analysis of Figure 1 but does not take into account the subsequent fate of the NO_2, which can itself react with oxyMb, ferrylMb, and NO as shown in Scheme 3.[14,34] Using the literature values of the rate constants for the Scheme 3 reactions, it is straightforward to predict the expected product distributions as a function of time (see Supporting Information). Figure 2 shows the calculated time evolution of all the species in Scheme 3, assuming initial concentrations [MbO_2] = 316 μM and [NO] = 86 μM, where the NO concentration is taken as equal to the amount of **1** photolyzed, as calculated from the Figure 1 fit. Notice that the Figure 2 calculations predict that, under the given experimental conditions, the reactions of NO_2 with the various Mb species will themselves result in a net *increase* in the ferrylMb concentration, so that after 10 ms the ferrylMb will reach ∼16 μM. Thus, the 5 μM ferrylMb calculated in the red trace analysis of Figure 1 is less than a third of that predicted for the reaction of oxyMb with NO, if one assumes that the reaction

dx.doi.org/10.1021/ic400697a | Inorg. Chem. 2013, 52, 7623−7632

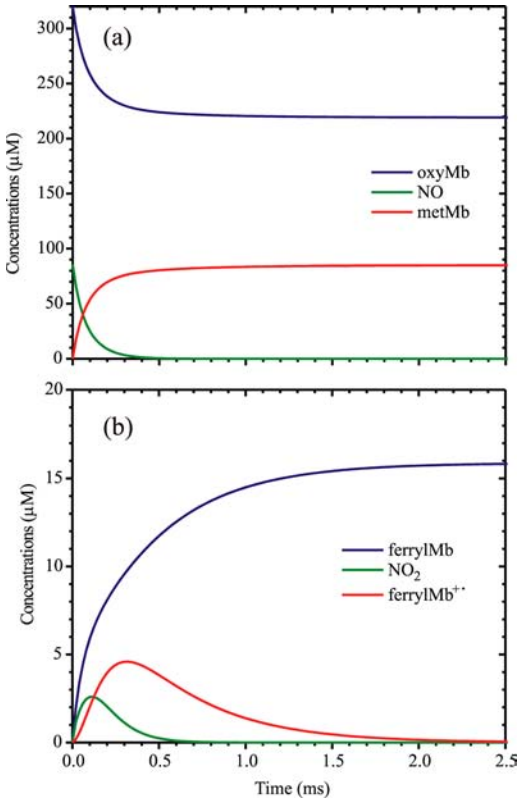

Figure 2. Time evolution of reactant and product concentrations that is expected following the reaction of 85.6 μM NO with 316 μM oxyMb (initial concentrations in the Figure 1 data), if one assumes a metMb(OONO) intermediate in common with the metMb + $ONOO^-$ reaction. Concentrations were calculated using numerical integration of the corresponding rate equations, and the known rate constants given in Scheme 3, as described in the Supporting Information. Panel a shows major species and panel b, minor ones.

goes via the same intermediate as the metMb-catalyzed peroxynitrite isomerization.[19]

Experiments in the Presence of Ascorbate. The result presented above places an upper bound on the amount of ferrylMb produced when NO is photogenerated from **1** in the presence of a large excess of oxyMb but leaves open the question of whether *any* ferrylMb is in fact produced. This is because the Figure 1 spectrum is equally well fitted if one assumes that Mb is a minority species instead of ferrylMb. Furthermore, the minor features in the residual trace of Figure 1 allow for the possibility that minority species other than Mb or ferrylMb are also contributing to the Figure 1 spectrum, and one cannot assess the significance of such species from analysis of single spectral traces such as Figure 1.

In order to more precisely quantify the amount of ferrylMb produced in the reaction of photogenerated NO with excess oxyMb, the Figure 1 experiment was repeated in the presence of varying amounts of ascorbate, with continued monitoring of the reaction solution over tens of seconds. FerrylMb reacts with ascorbate in a second-order process governed by a rate constant of 2.7 ± 0.8 M^{-1} s^{-1},[37] which should generate a readily detectable, ascorbate concentration-dependent kinetic fingerprint with a many-second lifetime. When a solution containing 272 μM oxyMb, 1.66 mM **1**, and 200 mM ascorbate was irradiated with a 500 nm laser pulse, an analysis analogous to that of Figure 1 above showed initial product distributions of either ΔC_{metMb} = 96 μM, ΔC_{oxyMb} = ΔC_1 = −100 μM, and $\Delta C_{ferrylMb}$ = 4 μM or ΔC_{metMb} = $-\Delta C_1$ = 97 μM, ΔC_{oxyMb}= −100 μM, and ΔC_{Mb} = 3 μM (see Supporting Information). The experiment was then followed for an additional 45 after the initial laser pulse, and double-difference spectra were generated by subtracting the first difference spectrum from every subsequent one. Figure 3a shows a number of these double-difference spectra, collected at selected times after the laser pulse and refined using singular value decomposition (see Supporting Information).[38,39] Figure 3b shows corresponding ΔA_λ vs time traces at selected wavelengths. The complete set of double-difference spectra, collected at varying times and wavelengths, can be fitted empirically using a model that builds the spectra from the known extinction coefficients of Mb, metMb, oxyMb,and species **1** and accounts for the time dependence of ΔA at each wavelength using eq 1. The detailed fitting procedure is described in the Supporting Information. Equation 1 shows that at any given wavelength two components contribute to the total absorbance change, one

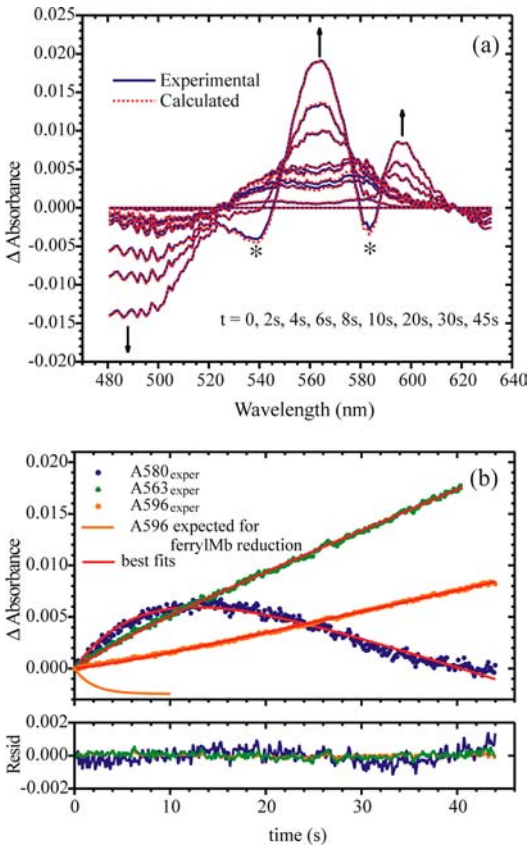

Figure 3. Spectral changes that follow irradiation of a solution initially containing 272 μM oxyMb, 1.72 mM **1**, and 200 mM ascorbate with a 500 nm laser pulse. (a) Double-difference spectra obtained by subtracting the first difference spectrum (equivalent to the Figure 1 spectrum) from all subsequent difference spectra that followed the laser pulse. The representative spectra shown here were collected 0, 2, 4, 6, 8, 10, 20, 30, and 45 s after the initial spectrum. Theoretical traces (dashed red lines) were calculated as described in the Supporting Information. Arrows indicate regions where spectral changes are monotonic, while stars indicate regions in which ΔA first increases and then decreases. (b) ΔA vs t slices at selected wavelengths, corresponding to the data shown in a. The short orange trace shows the absorbance change at 596 nm that would accompany the reduction of 4 μM ferrylMb to metMb by 0.2 M ascorbate.

dx.doi.org/10.1021/ic400697a | Inorg. Chem. 2013, 52, 7623−7632

varying linearly and the second exponentially with time. The parameter m_λ represents the rate of change

$$\Delta A_\lambda = m_\lambda t + \Delta A inf_\lambda (1 - e^{-kt}) \quad (1)$$

of the linear component (in ΔAU/s), while $\Delta A inf_\lambda$ and k represent the final amplitude and rate constant, respectively, for the exponential component. The calculated spectra and time traces are overlaid on the experimental data of Figure 3a and b. From the fitting procedure, the changes in concentration with time of Mb, metMb, oxyMb, and NO (indirectly obtained from the concentration change of **1**) were calculated; these are plotted in Figure 4. In addition, the value of the rate constant governing the exponential part of eq 1 was calculated to be k = 0.133 ± 0.005 s^{-1}.

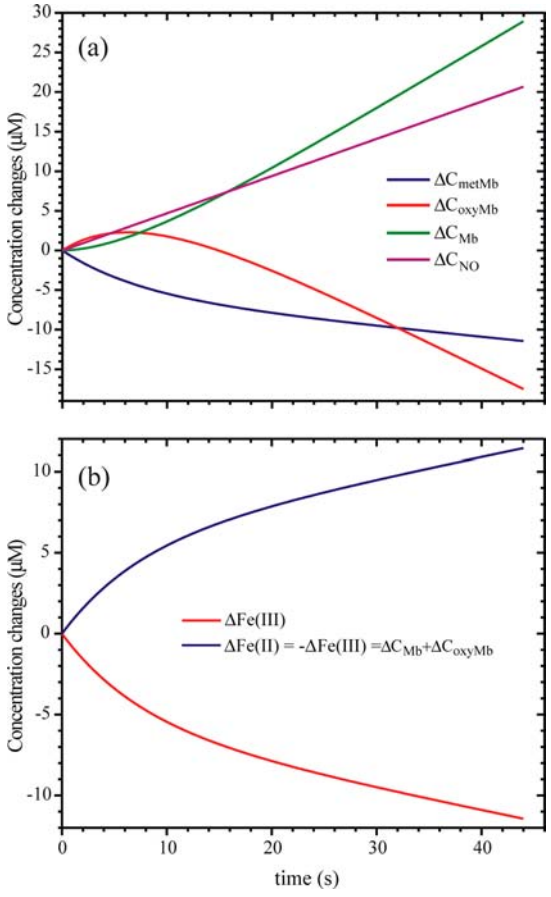

Figure 4. (a) Changes in concentration of the myoglobin species that gave rise to the spectral changes of Figure 2, calculated as described in the Supporting Information. Also shown is the increase in [NO] with time that was effected by photolysis of **1** in the spectrophotometer probe beam. This was calculated from the absorbance change that accompanied the denitrosylation of **1**. (b) Similar to a, this plot shows the total myoglobin reduced from the Fe(III) to the Fe(II) state as a function of time.

Given the 2.7 M^{-1} s^{-1} rate constant for the reaction of ferrylMb with ascorbate,[37] any ferrylMb present immediately after the laser pulse should have subsequently been reduced by the 200 mM ascorbate in a pseudo-first-order process with k_{obs} = 0.54 s^{-1}, which translates to a half-life of 1.3 s. The Figure 3 kinetic data show no evidence for such a kinetic process. If 4 μM of ferrylMb had in fact been present immediately after irradiating the reaction solution, as suggested by spectral analysis analogous to that which produced the red trace of Figure 1 (Supporting Information), it should then have reacted with ascorbate to generate metMb, giving rise to a detectable spectral signature with a maximum amplitude at 596 nm. Figure 3b compares the absorbance change expected from the reduction of ferrylMb to metMb with that actually observed at 596 nm. Though the predicted change is small, it should have been clearly resolvable given the low noise of the data obtained on this time scale (a conservative estimate suggests that 1−2 μM ferrylMb should have been detectable by the applied method; see Supporting Information for a statistical analysis). Furthermore, the theoretical analysis of Scheme 3 and Figure 2 predicts a spectral change that is ∼3−4 times larger. On the basis of the Figure 3 analysis, one can therefore conclude that ferrylMb is not present in detectable quantities (>1−2 μM) by the time the first postlaser flash spectra are collected, 16−160 ms after the laser pulse. Other minor species, such as Mb (e.g., green trace, Figure 1), may be present at this point.

The results presented in Figures 3 and 4 can be qualitatively explained on the basis of NO formed by the photolysis of **1** in the spectrophotometer probe beam and of the known reactivity of ascorbate with oxyMb and metMb that is outlined in Scheme 4.[19,37,40] The linear increase in NO concentration shown in

Scheme 4[a]

$$\text{metMb} + \text{AH}^- \longrightarrow \text{Mb} + \text{A}^{-\bullet} + \text{H}_2\text{O} + \text{H}^+ \quad (1)$$

$$\text{Mb} + \text{O}_2 \rightleftharpoons \text{oxyMb} \quad (2)$$

$$\text{oxyMb} + 3\text{AH}^- + \text{H}^+ \longrightarrow \text{metMb} + 3\text{A}^{-\bullet} + \text{H}_2\text{O} \quad (3)$$

[a]Here, AH^- is ascorbate, and $A^{-\bullet}$ is the ascorbyl radical. Two equivalents of H_2O are generated in step 3, one of which binds to Fe(III) in the metMb.

Figure 4 ($\Delta C_{NO}/\Delta t$ = 4.7 × 10^{-7} Ms^{-1}) arises from the photolysis of **1** by the spectrophotometer probe beam, as can be verified by submitting solutions of pure **1** to the same treatment (Supporting Information). The NO so generated will immediately react with oxyMb to produce metMb, thus contributing to the concentration changes of these two species. Step 3 of Scheme 4 is a second process that results in a net oxidation of oxyMb to metMb.[40] In this process, 1 equiv of ascorbate first reacts with oxyMb to generate metMb and H_2O_2.[40] The metMb and H_2O_2 then react to give the ferrylMb cation radical (ferrylMb$^{+\bullet}$, formally Mb with Fe(V)),[40,41] which is rapidly reduced by 2 equiv of ascorbate back to metMb. The net process of step 3 in Scheme 4 results in the four-electron reduction of O_2 to give 2 equiv of H_2O (one of which binds to the Fe of oxidized myoglobin), with three of the necessary electrons coming from ascorbate and 1 equiv from the myoglobin Fe(II). The 3 equiv of ascorbyl radicals generated in the process subsequently disproportionate.[37,40] Counteracting the net oxidation of oxyMb to metMb by NO and by step 3 of Scheme 4 is the reduction of metMb by ascorbate (step 1, Scheme 4). From experiments with metMb and ascorbate under anaerobic conditions, the second-order rate constant for this reaction is calculated to be 0.053 ± 0.002 M^{-1} s^{-1} at pH 7.4 (Supporting Information). This step initially generates Mb, but in the presence of O_2 the Mb is in equilibrium with oxyMb (step 2, Scheme 4).

Figure 4b shows that over the time period monitored there was a net reduction of Fe(III) (metMb) to Fe(II) (oxyMb and Mb) but that the rate of reduction slowed over time. Immediately after the laser pulse, the reaction mixture contains

dx.doi.org/10.1021/ic400697a | Inorg. Chem. 2013, 52, 7623−7632

roughly 97 μM metMb, 3 μM Mb, and 172 μM oxyMb (as determined by analysis analogous to that which produced the green trace of Figure 1; Supporting Information). Presumably, as metMb is subsequently consumed and reduced myoglobin is generated, the rates of the net oxidizing and net reducing processes move toward a dynamic equilibrium, beyond which no further changes in concentration would be observed. The distribution of reduced species also changes with time as seen in Figure 4a. Step 3 of Scheme 4 consumes oxygen, as does the reaction of oxyMb with NO, and in the small cuvette employed for the experiments the oxygen is not rapidly replaced by diffusion from the surroundings. Thus, over time, the concentration of oxyMb decreases and that of Mb increases. Experiments with solutions containing only oxyMb and ascorbate in the same type of cuvette showed the same general reactivity (Supporting Information), though the exact reaction conditions could not be reproduced in the absence of the laser pulse that rapidly consumed an initial quantity of O_2.

In addition to the experiment described above (Figures 3 and 4), similar experiments were also performed in the presence of 100 μM and 300 μM ascorbate (see Supporting Information). In all of these experiments, the time-resolved spectra lacked the kinetic fingerprint that would be expected if ferrylMb had been generated in the reaction of oxyMb with NO but were otherwise consistent with the expected reactivity of the reaction mixtures, as outlined in Scheme 4. Finally, to ensure that the reaction of ferrylMb with ascorbate is not altered under the specific reaction conditions employed in this study, authentic ferrylMb was reacted with ascorbate in the presence and absence of **1**, oxyMb, or Mb. In all cases, the same rate constant was obtained, which in turn agreed with the literature values (see Supporting Information).[19,37]

Stability of ferrylMb in the Presence of Species 1, with and without Laser Irradiation. The experiments presented above demonstrate conclusively that no ferrylMb is detectable 16 ms after irradiating solutions of oxyMb and **1** with a 500 nm laser pulse. However, they do not preclude the possibility that detectable amounts of ferrylMb were generated on the microsecond time scale but consumed prior to 16 ms in reactions specific to the conditions employed. In order to test for this possibility, several experiments were performed with authentic ferrylMb and **1**.

Figure 5 shows the spectral changes observed at 409 nm after mixing 4.2 μM ferrylMb with 238 μM **1**. The absorbance at 409 increases exponentially, indicating that the ferrylMb is being reduced to metMb with an apparent rate constant of 1.7×10^{-3} s^{-1}. When the experiment was repeated in the presence of half the concentration of **1**, the apparent rate constant also decreased by half, showing that the reduction is first order in [**1**] and second order overall. The value of the true second-order rate constant for reduction of ferrylMb in the presence of **1** is therefore ~7 M^{-1} s^{-1}. In the experiments with oxyMb and **1** described above, the concentration of **1** was typically between 1.5 and 2 mM; therefore one expects any ferrylMb generated under those conditions to be reduced with a half-life of ~50–65 s. This reaction is too slow to eliminate ferrylMb before it could be detected in the experiments of the previous sections; in particular it would not compete with the reaction of ferrylMb with 200 mM ascorbate, which is predicted to occur with a half-life of 1.3 s.

As shown in Scheme 3, NO reacts rapidly with ferrylMb. Thus, the spectral changes seen in solutions containing ferrylMb and **1** (Figure 5) could simply be due to the reaction

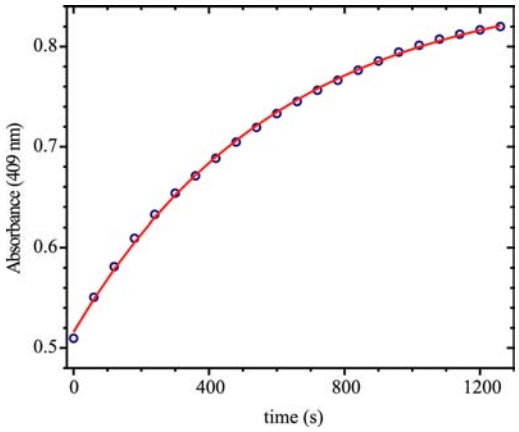

Figure 5. Spectral changes observed at 409 nm after mixing 4.2 μM ferrylMb with 238 μM **1**. Blue circles: experimental data. Red curve: theoretical fit to an exponential function.

between ferrylMb and NO photogenerated from **1** in the spectrometer probe beam. Alternatively, the $Mn(PaPy_2Q)H_2O^+$ that is cogenerated from the photolysis of **1** could also contribute to ferrylMb reduction. These possibilities were addressed in kinetic and stoichiometric studies. In the kinetic experiments, species **1** was photolyzed in the presence of varying amounts of ferrylMb, and the subsequent reactions were monitored on the microsecond time scale (Figure 6). These experiments were carried out under pseudo-first-order conditions, such that the concentration of ferrylMb greatly exceeded the amount of NO photogenerated in every

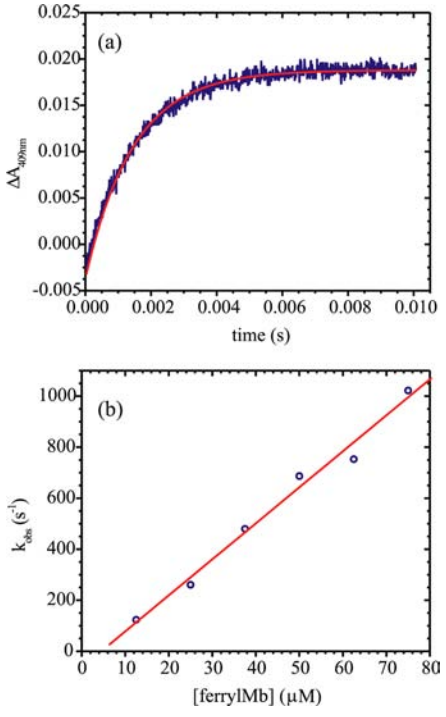

Figure 6. (a) Spectral changes observed at 409 nm after irradiating a solution containing 50 μM ferrylMb and 40 μM **1** with a 500 nm laser pulse. Blue trace: experimental data. Red trace: data fitted to a single exponential. (b) Dependence of the observed rate constant on [ferrylMb] when the experiment of part a was repeated with varying initial ferrylMb concentrations. In all cases, $[NO]_{generated} \ll [ferrylMb]_0$.

dx.doi.org/10.1021/ic400697a | Inorg. Chem. 2013, 52, 7623–7632

experiment. The change in absorbance at 409 nm with time was exponential at all ferrylMb concentrations (Figure 6a), and plots of k_{obs} vs [ferrylMb] were linear (Figure 6b), showing that the reaction was first-order in [ferrylMb] and second-order overall. The true second-order rate constant for the reaction was calculated to be $(1.4 \pm 0.1) \times 10^7$ M^{-1} s^{-1} from the slope of the Figure 6b line, a value that is close to that previously reported in the literature for the reaction between NO and ferrylMb (Scheme 3).[35]

The agreement between the rate constant calculated from Figure 6b and that reported earlier by Herold and Rehman[35] demonstrates that NO is the fastest reducing agent present in photolyzed mixtures of ferrylMb and **1**. If it were not, the rate constant calculated from Figure 6b would have been higher than Herold and Rehman's. The close agreement does not, however, exclude the possibility that $Mn(PaPy_2Q)H_2O^+$ also reduces ferrylMb at rates comparable to or lower than NO. To address this possible alternative, the amount of ferrylMb reduced and the amount of NO generated by photolysis of a given amount of **1** were determined independently, in a set of experiments that are described in Supporting Information. In these experiments, only one equivalent of ferrylMb was reduced per equivalent of **1** photolyzed, which shows that NO is the sole reducing agent generated in the photolysis. If $Mn(PaPy_2Q)H_2O^+$ were also capable of reducing ferrylMb on the subsecond time scale, two equivalents of ferrylMb would have been reduced per equivalent of **1** photolyzed in these experiments. Therefore, in the experiments in which solutions of oxyMb and **1** were irradiated to generate NO, free ferrylMb generated by homolytic fragmentation of a metMb(OONO) intermediate should have still been present 16 ms after photolysis, and thus detectable.

Evaluation of the Scheme 3 Model. Given that ferrylMb was not generated in detectable quantities in the present experiments, contrary to the predictions of earlier reports as outlined in Scheme 3, it is now necessary to assess the sensitivity of the Scheme 3 conclusions to possible errors in the published kinetic parameters. One question that immediately arises is whether Su and Groves could have overestimated the amount of cage escape (Scheme 1) that occurred in their experiments; the values of k_{11} and k_{12} in Scheme 3 are based directly on this estimate.[19] When the numerical simulation that they used to obtain the k_r/k_e estimate of 10 was repeated, this estimate was found to be very insensitive to even large variations in the inputted initial concentrations of metMb and peroxynitrite. Therefore, Su and Groves' estimate for *initial* ferrylMb generation via cage escape cannot be very far off.

Next to be examined were the possible effects that uncertainties in the Scheme 3 rate constants might have on the predicted time evolution of the ferrylMb concentration. Of all the parameters in Scheme 3, the one with the greatest reported uncertainty is k_6, for which the literature value is given as a range (10^4 M^{-1} s^{-1} to 10^7 M^{-1} s^{-1}).[14] For the calculations that yielded Figure 2, the upper bound was arbitrarily chosen (Supporting Information), but a smaller value of k_6 is unlikely to change the conclusions; if $ferrylMb^{+\bullet}$ reacts more slowly with oxyMb, then it is almost certainly still converted to ferrylMb by other competing processes, such as reduction by ascorbate.

The fact that $(k_{11} + k_{12})$ and k_2 are within 20% of the reported values[8,35] was independently verified herein (Supporting Information and Figure 6). Of the remaining parameters, k_3 and k_7 prove to be too small to have any real impact on the outcome of the simulations, given the reaction conditions being modeled. This leaves k_4, k_5, k_8, k_{-8}, and k_9 as parameters that could significantly affect the predicted time evolution of [ferrylMb].

The parameters k_4, k_5, k_8, k_{-8}, and k_9 all govern the fate of the NO_2 that putatively escapes the protein cage. Any increase in the ratio k_5/k_4 will lead to greater net recombination of ferrylMb with NO_2, thus decreasing the final amounts of both species. However, in practice it would take a huge error in the literature derived value of this ratio (0.267 from Scheme 3) to have any significant effect on ferrylMb survival under the reaction conditions being modeled, where at all times the oxyMb concentration far exceeded any ferrylMb that might be generated. Thus, for example, if the value of k_4 is decreased to 5×10^6 M^{-1} s^{-1} and that for k_5 is increased to 10^8 M^{-1} s^{-1} (both these numbers are well outside the reported uncertainties for the respective parameters), a simulation still predicts the presence of ~10 μM ferrylMb 10 ms after the laser pulse. A k_5 value of 10^8 M^{-1} s^{-1} for the ferrylMb reaction with NO_2 would make it by far the largest known rate constant for the reaction of NO_2 with a biomolecule,[14] while the k_4 value of 5×10^6 M^{-1} s^{-1} would be at the low end of values reported for the interaction of small gas molecules with either oxyMb or Mb.[8,14,42,43] And yet, much greater changes in the input rate constants would be needed to decrease the ferrylMb concentration below 1–2 μM (the estimated detection limit for these experiments).

The processes governed by k_8, k_{-8}, and k_9 determine the rate at which NO_2 is consumed independently of ferrylMb. The value of k_8 for the reaction of NO with NO_2 is at the diffusion limit and so is unlikely to be underestimated. However, if k_{-8} is overestimated and/or k_9 is underestimated in Scheme 3, then all else being equal the Figure 2 analysis would be overestimating the amount of ferrylMb that is eventually generated by reaction of NO_2 with oxyMb. Note however that even in the extreme case whereby *none* of the NO_2 resulted in additional ferrylMb formation, one would still see the 10% ferrylMb generated by the initial NO_2 cage escape, if this were occurring.

To summarize, even if one assumes much larger uncertainties in the kinetic parameters of Scheme 3 than are provided with the literature values, ferrylMb is predicted to accumulate to concentrations 5–10 times above the detection limit in the experiments presented herein, if the reactions of oxyMb with NO and metMb with peroxynitrite share a common metMb(OONO) intermediate, as proposed in Scheme 1.

■ DISCUSSION

Investigations by the Groves group and others over the past decade have shown fairly convincingly that, during metMb-catalyzed isomerization of peroxynitrite, some nitration of Tyr103 from the metMb takes place, and ferrylMb builds up as a transient but detectable intermediate.[12,17,19] These results are consistent with the mechanism of Scheme 1 path 2, whereby peroxynitrite first binds the Fe heme center to produce a metMb(OONO) intermediate, which then rapidly cleaves homolytically to form ferrylMb and caged NO_2. The NO_2 can then either recombine with the ferrylMb to release nitrate, or escape the cage; the latter path gives rise to the ferrylMb that is transiently detectable, and to the observed Tyr103 nitration. In an early report, the extent of cage escape was estimated to be as high as 20%,[17] but this was later revised downward to ~10%.[19]

dx.doi.org/10.1021/ic400697a | Inorg. Chem. 2013, 52, 7623–7632

It has been widely assumed until now that the reaction between oxyMb and NO proceeds through the same metMb(OONO) intermediate as the reaction between metMb and peroxynitrite (Scheme 1); however, if this assumption is correct, then under appropriate conditions one should be able to detect the ferrylMb side product due to 10% cage escape of NO_2, as Groves' group did when reacting peroxynitrite with metMb.[19] The fact that this intermediate was not detected in any of the experiments presented herein calls the assumption into question. In this regard, the key experiments are those performed in the presence of ascorbate (Figures 3, 4 and Supporting Information). Single spectrum analyses such as that given in Figure 1 are of limited use because all of the components contributing to such a spectrum may not be known. However, the kinetic analyses of the ascorbate experiments are substantially more sensitive to ferrylMb concentration and relatively insensitive to the effects of unknown parameters. No matter what species are contributing to the overall spectra, any spectral *changes* due to conversion of ferrylMb to metMb should have been readily detectable if ferrylMb concentrations greater than 1−2 μM had been produced from the reaction between oxyMb and photogenerated NO. This is clear from inspection of the short orange trace in Figure 3b, which shows the spectral change at one representative wavelength that would be associated with the conversion of 4 μM ferrylMb to metMb in the presence of 200 mM ascorbate. However, 4 μM is only the largest amount of ferrylMb consistent with analysis of the t_0 spectrum for the data set (the analogue of the Figure 1 spectrum; see Supporting Information). If the reaction of oxyMb with NO had produced 10% ferrylMb, as predicted from the experiments with metMb and peroxynitrite, the amplitude of the Figure 3 short orange trace should have been at least twice as large, and according to the extended analysis based on Scheme 3 it could have been as much as 4 times greater. Furthermore, the short orange trace of Figure 3 is only for one wavelength. The analysis presented herein was a global one, and the expected kinetic signature for ferrylMb reduction to metMb was absent from the entire monitored spectral region (480−620 nm). The same was true in experiments with 100 mM and 300 mM ascorbate (see Supporting Information).

The experiments with ferrylMb and **1** (Figures 5 and 6 and Supporting Information) show that neither **1** nor its photoproduct $Mn(PaPy_2Q)H_2O^+$ will react with ferrylMb in less than 1 s, so if this species had been generated from oxyMb and NO it should have persisted long enough to react with ascorbate on the time scale of seconds. Furthermore, the experiments with ferrylMb and ascorbate show that the kinetics of this crucial reaction were unaffected by the specifics of the reaction conditions (see Supporting Information). Together, the experiments with ferrylMb confirm that this transient species should have been detectable if it had been generated in the quantities predicted from experiments with metMb and peroxynitrite,[17,19] via path 2 of Scheme 1.

Scheme 5 proposes one reaction mechanism for oxyMb + NO that would yield a product distribution different from that obtained in the reaction between metMb and peroxynitrite. In this scenario, NO directly inserts into the oxyMb O−O bond, thus completely bypassing the metMb(OONO) intermediate. Some model studies with synthetic iron porphyrin complexes support the hypothesis that different mechanisms may operate in reactions of ferric porphyrins with peroxynitrite and in reactions of oxyferrous porphyrins with NO. For example,

Scheme 5

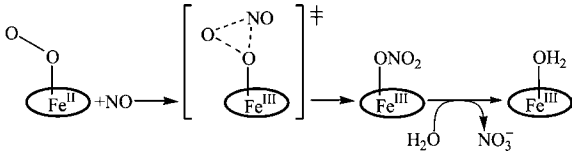

Kurtikyan and Ford recently reported careful studies in which synthetic complexes with the formula $Fe(Por)(NH_3)(O_2)$, sublimed in vacuo onto liquid nitrogen-cooled CaF_2 or KBr surfaces, were exposed to NO gas.[44] Even in these low-temperature studies, the first detectable intermediate as the surface warmed up was invariably the nitrate adduct. From these studies, Kurtikyan and Ford concluded that if peroxynitrite intermediates actually formed, subsequent barriers for their isomerization to nitrate species were at most ∼7 kcal/mol.[44] By contrast, Lee et al. had shown earlier that some water-soluble Fe(III)porphyrins react with peroxynitrite to generate very long-lived oxoFe(IV) species and NO_2, that only slowly recombine.[45] The Kurtikyan and Lee experimental conditions are very different (hydrophobic porphyrins adsorbed on surfaces vs water-soluble porphyrins in aqueous solution), and this alone could explain the different product distributions. Alternatively it is also possible that the Kurtikyan and Ford reactions proceeded via a mechanism akin to Scheme 5, while those of Lee et al. followed path 2 of Scheme 1. It should be noted that Kurtikyan and co-workers *did*, very recently, detect the cobalt equivalent of a peroxynitrite-bound species and later NO_2, when they reacted synthetic oxy-coboglobin models with NO, using the surface deposition methodology summarized above.[46] Also, Schopfer and co-workers have reported indirect evidence that synthetic $Fe(Por)(NH_3)(O_2)$ complexes can react with NO via a pathway akin to that shown in Scheme 1, path 2. When tetrahydrofuran (THF) solutions containing tyrosine mimic 2,4-di-*tert*-butylphenol, and oxyMb mimic $(THF)(F_8)Fe^{III}(O_2^{+\bullet})$ [where F_8 = tetrakis(2,6-difluorophenyl)porphyrinate(2-)], were exposed to NO, the nitrated product 2,4-di-*tert*-butyl-6-nitrophenol was recovered, as would be expected if free NO_2 was being formed from fragmentation of a peroxynitrite intermediate.[20] Schopfer et al. did not directly observe such an intermediate, but their experiments show that the question is far from settled.

Scheme 6 suggests an alternative to Scheme 5 that would also allow the reaction mechanism for oxyMb + NO to deviate from that of metMb + peroxynitrite but would not preclude a metMb(OONO) transient species in either case. In this scenario, the metMb(OONO) moiety itself is formed in both reactions and fragments homolytically to release NO_2 into the immediate surroundings of the heme, but the conformation of the protein surrounding the heme center is assumed to be significantly different in the two cases. This is depicted in Scheme 6 by representing the Fe(II)-derived protein conformation by a rectangle surrounding the heme moiety and that for Fe(III) by an ellipse. If the conformation of the protein derived from metMb were "leakier" than that derived from oxyMb ($k_{e2} \gg k_{e1}$ in Scheme 6), this would explain why ferrylMb and NO_2 are produced in the former case and not the latter. Using the most conservative estimate of the detection limit in the ascorbate experiments (∼2 μM), this mechanism would predict that k_{e2} in Scheme 6 is at least 10 times greater than k_{e1}.

dx.doi.org/10.1021/ic400697a | *Inorg. Chem.* 2013, 52, 7623−7632

Scheme 6

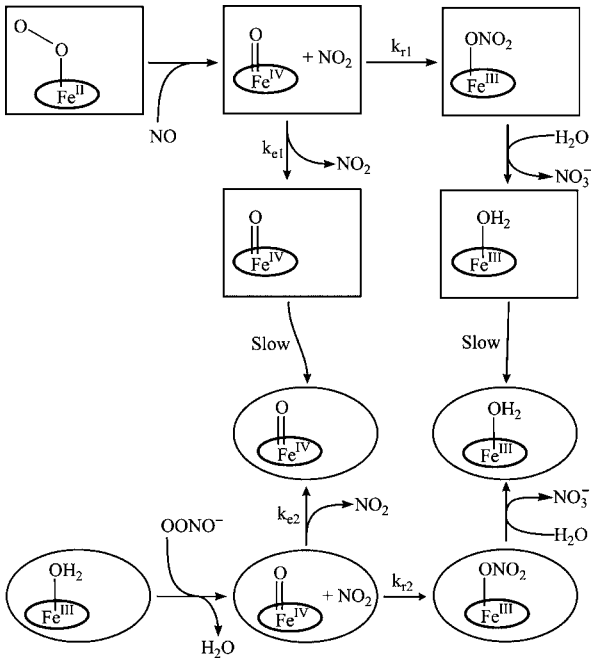

The fact that the reaction of oxyMb with NO gives different product distributions than that of metMb with peroxynitrite has important implications for researchers investigating the possible physiological role of myoglobin and related molecules as NO sinks. Path 2 of Scheme 1, which has now been identified as the likely mechanism for metMb-catalyzed isomerization of peroxynitrite,[19] allows a significant amount of free NO_2 to escape the protein and concomitantly results in formation of ferrylMb. If NO dioxygenation by oxyMb were to follow exactly the same path, then removal of the reactive NO would be accompanied by generation of NO_2 and ferrylMb, which in many ways are at least as reactive. In contrast, the results of this investigation show that oxyMb converts NO to NO_3^- without generating any detectable ferrylMb side product. This makes a physiological role for myoglobin's NO dioxygenase activity that much more plausible.

■ ASSOCIATED CONTENT

Supporting Information

Determination of the rate constant for the reaction of metMb with ascorbate. The reaction of oxyMb with ascorbate. The reaction of ferrylMb with ascorbate. Laser photoinitiated fragmentation of species **1** in the absence of protein. Expected result of mixing 100 μM NO with 272 μM oxyMb, if the reaction of oxyMb with NO shared an intermediate with the metMb-catalyzed isomerization of peroxynitrite: a numerical simulation of the product distribution's evolution during the first 3 ms. Laser photoinitiated reaction of NO with excess oxyMb in the presence and absence of ascorbate: analysis of the data. Monitoring the reaction of oxyMb with NO on the microsecond time scale. Stability of ferrylMb in the presence of species **1** after laser irradiation: stoichiometric analysis. Statistical analysis of ferrylMb concentration in the reaction of oxyMb with NO at low ascorbate concentrations and in control experiments. This material is available free of charge via the Internet at http://pubs.acs.org.

■ AUTHOR INFORMATION

Corresponding Author

*Phone: (414)-229-4413. E-mail: apacheco@uwm.edu.

Present Address

[†]Department of Material Science and Engineering, Penn State University, 322 Steidle Building, University Park, PA 16802.

Notes

The authors declare no competing financial interest.

■ ACKNOWLEDGMENTS

This work was supported by grants UWM RGI 101X157, UWM RGI 101X225, and NSF 0843459. D.J.P. gratefully acknowledges support from the University of Wisconsin's Office of Undergraduate Research. The authors gratefully acknowledge Prof. Graham Moran for the use of his stopped-flow apparatus.

■ REFERENCES

(1) Wittenberg, J. B.; Wittenberg, B. A. *Annu. Rev. Biophys. Biophys. Chem.* **1990**, *19*, 217.
(2) Takahashi, E.; Endoh, H.; Doi, K. *Biophys. J.* **2000**, *78*, 3252.
(3) Garry, D. J.; Ordway, G. A.; Lorenz, J. N.; Radford, N. B.; Chin, E. R.; Grange, R. W.; Bassel-Duby, R.; Williams, R. S. *Nature* **1998**, *395*, 905.
(4) Brunori, M. *Trends Biochem. Sci.* **2001**, *26*, 209.
(5) Frauenfelder, H.; McMmahon, B. H.; Austin, R. H.; Chu, K.; Groves, J. T. *Proc. Natl. Acad. Sci. U. S. A.* **2001**, *98*, 2370.
(6) Hendgen-Cotta, U. B.; Merx, M. W.; Shiva, S.; Schmidz, J.; Becher, S.; Klare, J. P.; Steinhoff, H.-J.; Goedecke, A.; Schrader, J.; Gladwin, M. T.; Kelm, M.; Rassaf, T. *Proc. Natl. Acad. Sci. U. S. A.* **2008**, *105*, 10256.
(7) Cossins, A.; Berenbrink, M. *Nature* **2008**, *454*, 416.
(8) Herold, S.; Exner, M.; Nauser, T. *Biochemistry* **2001**, *40*, 3385.
(9) Moncada, S.; Palmer, R. M. J.; Higgs, E. A. *Pharmacol. Rev.* **1991**, *43*, 109.
(10) *Nitric Oxide, Principles and Actions*; Lancaster, J., Ed.; Academic Press: San Diego, CA, 1996.
(11) Ford, P. C.; Lorkovic, I. M. *Chem. Rev.* **2002**, *102*, 993.
(12) Su, J.; Groves, J. T. *Inorg. Chem.* **2010**, *49*, 6317.
(13) Olson, J. S.; Foley, E. W.; Rogge, C.; Tsai, A. L.; Doyle, M. P.; Lemon, D. D. *Free Radic. Biol. Med.* **2004**, *36*, 685.
(14) Goldstein, S.; Merenyi, G.; Samuni, A. *J. Am. Chem. Soc.* **2004**, *126*, 15694.
(15) Yukl, E. T.; de Vries, S.; Moenne-Loccoz, P. *J. Am. Chem. Soc.* **2009**, *131*, 7234.
(16) Gardner, P. R.; Gardner, A. M.; Martin, L. A.; Salzman, A. L. *Proc. Natl. Acad. Sci. U. S. A.* **1998**, *95*, 10378.
(17) Bourassa, J. L.; Ives, E. P.; Marqueling, A. L.; Shimanovich, R.; Groves, J. T. *J. Am. Chem. Soc.* **2001**, *123*, 5142.
(18) Herold, S.; Shivashankar, K. *Biochemistry* **2003**, *42*, 14036.
(19) Su, J.; Groves, J. T. *J. Am. Chem. Soc.* **2009**, *131*, 12979.
(20) Schopfer, M. P.; Mondal, B.; Lee, D.-H.; Sarjeant, A. A. N.; Karlin, K. D. *J. Am. Chem. Soc.* **2009**, *131*, 11304.
(21) Herold, S.; Shivashankar, K.; Mehl, M. *Biochemistry* **2002**, *41*, 13460.
(22) Purwar, N.; McGarry, J. M.; Kostera, J.; Pacheco, A. A.; Schmidt, M. *Biochemistry* **2011**, *50*, 4491.
(23) Eroy-Reveles, A.; Leung, Y.; Beavers, C. M.; Olmstead, M. M.; Mascharak, P. K. *J. Am. Chem. Soc.* **2008**, *130*, 4447.
(24) Drago, R. S.; Paulik, F. E. *J. Am. Chem. Soc.* **1960**, *82*, 96.
(25) Maragos, C. M.; Morley, D.; Wink, D. A.; Dunams, T. M.; Saavedra, J. E.; Hoffman, A.; Bove, A. A.; Isaac, L.; Hrabie, J. A.; Keefer, L. K. *J. Med. Chem.* **1991**, *34*, 3242.
(26) Atkinson, S. J.; Mowat, C. G.; Reid, G. A.; Chapman, S. K. *FEBS Lett.* **2007**, *581*, 3805.

(27) Cabail, M. Z.; Lace, P. J.; Uselding, J.; Pacheco, A. A. *J. Photochem. Photobiol. A* **2002**, *152*, 109.
(28) Cabail, M. Z.; Moua, V.; Bae, E.; Meyer, A.; Pacheco, A. A. *J. Phys. Chem. A* **2007**, *111*, 1207.
(29) Kostera, J.; Youngblut, M. D.; Slosarczyk, J. M.; Pacheco, A. A. *J. Biol. Inorg. Chem.* **2008**, *13*, 1073.
(30) Kostera, J.; McGarry, J. M.; Pacheco, A. A. *Biochemistry* **2010**, *49*, 8546.
(31) Youngblut, M.; Judd, E. T.; Srajer, V.; Sayyed, B.; Goelzer, T.; Elliott, S. J.; Schmidt, M.; Pacheco, A. A. *J. Biol. Inorg. Chem.* **2012**, *17*, 647.
(32) DeRosa, F.; Bu, X.; Ford, P. C. *Inorg. Chem.* **2005**, *44*, 4157.
(33) Bourassa, J.; DeGraff, W.; Kudo, S.; Wink, D. A.; Mitchell, J. B.; Ford, P. C. *J. Am. Chem. Soc.* **1997**, *119*, 2853.
(34) Goldstein, S.; Czapski, G. *J. Am. Chem. Soc.* **1995**, *117*, 12078.
(35) Herold, S.; Rehmann, F.-J. K. *J. Biol. Inorg. Chem.* **2001**, *6*, 543.
(36) Laverman, L. E.; Wanat, A.; Oszajca, J.; Stochel, G.; Ford, P. C.; van Eldik, R. *J. Am. Chem. Soc.* **2001**, *123*, 285.
(37) Kroger-Ohlsen, M.; Skibsted, L. H. *J. Agric. Food Chem.* **1997**, *45*, 668.
(38) Press, W. H.; Teukolsky, S. A.; Vetterling, W. T.; Flannery, B. P. *Numerical Recipes: The Art of Scientific Computing*, 3rd ed.; Cambridge University Press: New York, 2007; p 65.
(39) Henry, E. R.; Hofrichter, J. In *Meth. Enzymol.*; Brand, L., Johnson, M. L., Eds.; Academic Press: San Diego, CA, 1992; Vol. *210*, p 129.
(40) Giulivi, C.; Cadenas, E. *FEBS* **1993**, *332*, 287.
(41) Fenwick, C.; Marmor, S.; Govindaraju, K.; English, A. M.; Wishart, J. F.; Sun, J. *J. Am. Chem. Soc.* **1994**, *116*, 3169.
(42) Jameson, G. B.; Ibers, J. A. In *Biological Inorganic Chemistry*; Bertini, I., Gray, H. B., Stiefel, E. I., Valentine, J. S., Eds.; University Science Books: Sausalito, CA, 2007; p 363.
(43) Hoshino, M.; Maeda, M.; Konishi, R.; Seki, H.; Ford, P. C. *J. Am. Chem. Soc.* **1996**, *118*, 5702.
(44) Kurtikyan, T. S.; Ford, P. C. *Chem. Commun.* **2010**, *46*, 8570.
(45) Lee, J.; Hunt, J. A.; Groves, J. T. *J. Am. Chem. Soc.* **1998**, *120*, 7493.
(46) Kurtikyan, T. S.; Eksuzyan, S. R.; Hayrapetyan, V. A.; Martirosyan, G. G.; Hovhannisyan, G. S.; Goodwin, J. A. *J. Am. Chem. Soc.* **2012**, *134*, 13861.